Metabolomic changes in human adipose tissue derived products following non-enzymatic microfacturing

M. GARCIA-CONTRERAS[1,2], F. MESSAGGIO[1,2], A. J. MENDEZ[1] AND C. RICORDI[1,2]

[1]Diabetes Research Institute, University of Miami, Miller School of Medicine, Miami, FL, USA
[2]Ri.Med Foundation, Palermo, Italy

Abstract. – **OBJECTIVE:** In this study, we evaluated the metabolomic profiling of cryopreserved Lipogems® tissue products and the initial lipoaspirates before microfracturing, to determine altered metabolites that could result from the non-enzymatic processing or the cryopreservation method.

MATERIALS AND METHODS: Human Lipoaspirate samples (n=10) were divided in two aliquots, of which one was non-processed and the other was processed by Lipogems® device. Non-processed lipoaspirates and Lipogems® processed tissues were stored at -80°C fresh frozen (N=3 per group) or in the presence of 0.5 M dimethyl sulfoxide (DMSO) (N=7 per group). A global non-targeted metabolic profile on these samples was performed.

RESULTS: Differences were observed in carbohydrate and nucleotide metabolism. These alterations translated in long chain and polyunsaturated fatty acid levels and amino acid metabolites showed divergent trends. When Lipogems® and Lipoaspirate tissue products were cryopreserved with DMSO, amino acids tended to increase in Lipogems® product. However, in the absence of DMSO aminoacids and their catabolites, tended to decrease in Lipogems® fat tissue product.

CONCLUSIONS: Microfractured human adipose tissue has been shown to provide a more effective source of adult stromal cells compared to the initial lipoaspirated tissue material. These could be, according to our findings, due to the changes in the metabolic profile of lipoaspirate tissues products.

Key Words
Adipose tissue, Lipoaspirates, Non-enzymatic isolation, Metabolomic.

Introduction

Human adipose tissue it is known to be a significant reservoir of human adipose-derived mesenchymal stromal cells (hADSCs)[1]. hADSCs have a strong paracrine potential[2-4], which could favor native tissue regeneration and repair, making them a suitable option for regenerative cell-based therapies[5,6,7].

Among mesenchymal stromal cell sources, lipoaspirated adipose tissue is an ideal source because of its relative abundance and easy access compared to other sources[8]. Adipose tissue could also be banked and then used at future times for clinical applications[8,9]. Cryopreservation can be done with or without the addition of cryoprotective agents such as dimethyl sulphoxide (DMSO)[10]. To avoid some of the regulatory complexity and cost associated with enzymatically processed adipose tissue products and their *ex-vivo* expanded hADSCs, novel minimal manipulated adipose tissue products have been developed[11,12]. Mechanical methods provide a low cost, rapid and simple alternative to the use of enzymes for adipose tissue processing. Microfragmented lipoaspirates prepared using the Lipogems® system are enriched in hADSCs and pericytes[13,14] and have been successfully used clinically for several regenerative medicine applications[15-18].

In the present study, we investigated the effect of microfracturing adipose tissue from lipoaspirates and the effect of the use of DMSO in the cryopreservation procedure on the respective metabolomic profiles.

Materials and Methods

Ethics Statement

This study was approved by the Institutional Review Board (IRB) of the University of Miami. Subjects were enrolled at Top Body Sculpting Rejuvenation Center (Weston, FL, USA) upon previous informed consent signature. All specimens were negative for HIV (Human Immunodeficiency Virus 1 and 2), HCV (Hepatitis C Virus), HBV (Hepatitis B Virus) and cytomegalovirus.

Sample Collection and Processing

10 human adipose tissue samples were obtained from elective liposuction procedures under local anesthesia (Table I). Lipoaspirates were divided in two aliquots, of which one was non-processed and the other was processed by Lipogems® device as previously described[12] by the Lipogems® system, a non-enzymatic processing method consisting in a two step tissue cluster reduction which includes an emulsification step for reduction of oil and blood residues. Non-processed lipoaspirates and Lipogems® processed tissues were stored at -80°C fresh frozen (N=3 per group) or in the presence of 0.5 M dimethyl sulfoxide (DMSO) (N=7 per group) in alpha-MEM supplemented with 10% fetal bovine serum (FBS).

Metabolomic Analysis

Metabolite Analysis

The untargeted metabolomics profiling of lipoaspirate and Lipogems® tissues stored in the 0.5M DMSO absence or fresh frozen tissues was performed by Metabolon (Durham, NC, USA), according to published methods[19,20].

Sample Preparation

Samples were thawed only once and prepared using the automated MicroLab STAR® system from Hamilton Company (Reno, NV, USA). Several recovery standards were added prior to the first step in the extraction process for quality control (QC) purposes. To remove protein, dissociate small molecules bound to protein or trapped in the precipitated protein matrix, and to recover chemically diverse metabolites, proteins were precipitated with methanol under vigorous shaking for 2 min (Glen Mills GenoGrinder 2000, OPS Diagnostics, NJ,

USA) followed by centrifugation. The resulting extracted samples were dried and then reconstituted in solvents compatible to each of the following methods. Samples were divided into five fractions: two for analysis by two separate reverse phase (RP)/UPLC-MS/MS methods with positive ion mode electrospray ionization (ESI), one for analysis by RP/UPLC-MS/MS with negative ion mode ESI, one for analysis by HILIC/UPLC- MS/MS with negative ion mode ESI, and one sample was reserved for backup. Samples were placed briefly on a TurboVap® (Zymark) to remove the organic solvent. The sample extracts were stored overnight under nitrogen before preparation for analysis.

Ultrahigh Performance Liquid Chromatography-Tandem Mass Spectroscopy (UPLC-MS/MS)

All methods utilized a Waters ACQUITY ultra-performance liquid chromatography (UPLC) and a Thermo Scientific Q-Exactive high resolution/accurate mass spectrometer interfaced with a heated electrospray ionization (HESI-II) source and Orbitrap mass analyzer operated at 35,000 mass resolution. The sample extract was dried and then reconstituted in solvents compatible to each of the four methods. Each reconstitution solvent contained a series of standards at fixed concentrations to ensure injection and chromatographic consistency. One aliquot was analyzed using acidic positive ion conditions, chromatographically optimized for more hydrophilic compounds. In this method, the extract was gradient eluted from a C18 column (Waters UPLC BEH C18- 2.1x100 mm, 1.7 μm) using water and methanol, containing 0.05% perfluoropentanoic acid (PFPA) and 0.1% formic acid (FA). Another aliquot was also analyzed using acidic positive ion conditions; however, it was chromatographically optimized for more hydrophobic compounds. In this method, the extract was gradient eluted from the same afore mentioned C18 column using methanol, acetonitrile, water, 0.05% PFPA and 0.01% FA and was operated at an overall higher organic content. Another aliquot was analyzed using basic negative ion optimized conditions using a separate dedicated C18 column. The basic extracts were gradient eluted from the column using methanol and water, however with 6.5 mM ammonium bicarbonate at pH 8. The fourth aliquot was analyzed via negative ionization following elution from a HILIC column (Waters UPLC BEH Amide 2.1x150 mm, 1.7 μm) using a gradient consisting of water and acetonitrile

Table I. Subjects Information.

Sample	Age	Gender	Height (ft, in)	Weight (lbs)
Donor 1	26	Female	5'3"	148
Donor 2	26	Female	5'3"	145
Donor 3	29	Female	5'1"	132
Donor 4	33	Female	5'0"	151.6
Donor 5	53	Female	5'5"	234
Donor 6	33	Female	5'7"	156.2
Donor 7	42	Female	5'5"	251
Donor 8	25	Female	4'1"	130.2
Donor 9	30	Female	5'4"	120
Donor 10	21	Female	5'4"	120

with 10 mM ammonium formate, pH 10.8. The MS analysis alternated between MS and data-dependent MSn scans using dynamic exclusion. The scan range varied slighted between methods but covered 70-1000 m/z. Raw data files were archived and extracted as described below.

Data Extraction and Compound Identification

Raw data was extracted, peak-identified and QC processed using Metabolon's hardware and software. These systems are built on a web-service platform utilizing Microsofts NET technologies, which run on high-performance application servers and fiber-channel storage arrays in clusters to provide active failover and load-balancing. Compounds were identified by comparison to library entries of purified standards or recurrent unknown entities. Metabolon maintains a library based on authenticated standards that contain the retention time/index (RI), mass to charge ratio (m/z), and chromatographic data (including MS/MS spectral data) on all molecules present in the library. Furthermore, biochemical identifications are based on three criteria: retention index within a narrow RI window of the proposed identification, accurate mass match to the library ± 10 ppm, and the MS/MS forward and reverse scores between the experimental data and authentic standards. The MS/MS scores are based on a comparison of the ions present in the experimental spectrum to the ions present in the library spectrum. Peaks were quantified using area-under-the-curve. For studies spanning multiple days, a data normalization step was performed to correct variation resulting from instrument inter-day tuning differences. Essentially, each compound was corrected in run-day blocks by registering the medians to equal one (1.00) and normalizing each data point proportionately.

Data analysis

Data were elaborated by using the random forest (RF) analysis, developed by Breiman[21]. For a given decision tree, a random subset of the data with identifying true class information is selected to build the tree ("bootstrap sample" or "training set"), and then the remaining data, the "out-of-bag" (OOB) variables, are passed down the tree to obtain a class prediction for each sample. The final classification of each sample is determined by computing the class prediction frequency ("votes") for the OOB variables over the whole forest. To determine which variables (biochemicals) make the largest contribution to the classification, a "variable importance" measure is computed. We use the "Mean Decrease Accuracy" (MDA) as this metric. The MDA is determined by randomly permuting a variable, running the observed values through the trees, and then reassessing the prediction accuracy.

Principal component analysis (PCA) was performed on the 409 log-transformed metabolites to provide a high-level overview of variation in the dataset. Component scores were calculated by using the standardized scoring coefficient.

To visualize interaction networks and biological pathways of the significant metabolites, we utilized Cytoscape (http://cyto- scape.org), an open source software platform[22].

Statistical Analysis

Statistical analysis of log-transformed data was performed using "R" version 2.14 (http://cran.r-project.org/), which is a freely available, open-source software package.

Following log transformation and imputation of missing values, if any, with the minimum observed value for each compound, Welch's two-sample *t*-test was used to identify biochemicals that differed significantly between experimental groups. Multiple comparisons were accounted for by estimating the false discovery rate (FDR) using q- values. Biochemicals were considered statistical significance when *p*-value ≤ 0.05 and those approaching significance 0.05<*p*-value<0.10 were considered to have trending changes.

Results

Metabolic Data overview

Following data acquisition and curation of a 409 compounds (named biochemicals) were identified. Following log transformation and imputation of values below the level of detection, if any, with the minimum observed value for each compound, Welch's two- sample *t*-test was used to identify biochemicals that differed significantly between no DMSO and DMSO groups. In Lipoaspirate no DMSO *vs.* Lipoaspirate DMSO, the levels of 201 biochemicals were significantly different between no DMSO and DMSO groups (*p*-value<0.05), 173 biochemicals were increased and 28 decreased. In Lipogems® no DMSO and Lipogems® DMSO 242 biochemicals were significantly different between no DMSO and DMSO groups (*p*<0.05), 209 biochemicals were increased

Table II. Summary of biochemical alterations induced by adipose microfracturing from a total of 409 named biochemicals identified.

| Statistical Comparisons		
Welch's Two-Sample *t*-Test	**No DMSO Lipogems® vs. DMSO Lipogems®**	**No DMSO Lipoaspirate vs. DMSO Lipoaspirate**
Total biochemicals $p \leq 0.05$ Biochemicals	242	201
(↑↓)	33 | 209	28 | 173
Total biochemicals $0.05<p<0.10$ Biochemicals	29	40
(↑↓)	15 | 14	19 | 21
Matched Pairs *t*-Test	**DMSO Lipogems® vs DMSO Lipoaspirate**	**No DMSO Lipogems® vs.No DMSO Lipoaspirate**
Total biochemicals $p \leq 0.05$ Biochemicals	246	112
(↑↓)	95 | 151	1 | 111
Total biochemicals $0.05<p<0.10$ Biochemicals	34	25
(↑↓)	18 | 16	2 | 23

and 33 decreased. In addition, there were a similar number of biochemicals which demonstrated a trend ($0.05<p$-value<0.10) toward significance in these analyses (Table II). Matched pairs *t*-test was used to identify biochemicals that differed significantly between Lipoaspirate and Lipogems® groups. In Lipoaspirate DMSO *vs.* Lipogems® DMSO the levels of 246 biochemicals were different between Lipoaspirate and Lipogems® groups (p-value < 0.05), 95 biochemicals were increased and 151 decreased. In Lipoaspirate no DMSO *vs.* Lipogems® no DMSO 112 biochemicals were significantly different between Lipoaspirate and Lipogems® groups (p-value<0.05), 1 biochemical was increased and 111 decreased. In addition, there were a similar number of biochemical, which achieved a trend value ($0.05<p$-value<0.10) toward significance in these analyses (Table II).

In the Principal Component Analysis (PCA) (which gives a value to each biochemical to show contributions to the Component scores) (Figure 1 A) Component 1 is correlated with the presence or absence of DMSO, suggesting this was the greatest source of variation in the dataset. Component 2 separated between Lipoaspirate and Lipogems®, which may reflect differences due to the microfracturing process. In the hierarchical clustering analysis (HCA) (Figure 1 C), which assesses sample similarity, samples tended to cluster well, with the top-level split in the dendrogram separating between DMSO and fresh frozen samples. The PCA Loadings plot (Figure 1B) separates the biochemicals separating groups in the PCA. Lipids tended to move northward in the loadings plot, which could suggest enrichment in the lipoaspirate samples. Enrichment for the vascular niche (and associated Mesenchymal stem cells) may lead to loss of adipocytes from the sample, which could be consistent with declines in lipid metabolites. However, lipids tended to move rightward in Component 1, which could reflect DMSO function as detergent. Several xenobiotics and nucleotide metabolites (adenine and uridine) also showed changes associated with processing; changes in carbohydrate metabolites (e.g., 3-phosphoglycerate) were also observed.

Carbohydrate Metabolism

Glucose can be utilized to support a variety of physiological processes, including energy generation, fatty acid synthesis, protein glycosylation, and nucleotide biogenesis. Metabolomic profiling revealed in No DMSO fresh frozen Lipogems® *vs.* Lipoaspirate, glucose and related products (e.g., 3-phosphoglycerate, phosphoenolpyruvate) a decreased, which could suggest high demand for use. However, the glycolytic end- products pyruvate and lactate were not significantly changed, but did show a non- significant decline. A similar phenotype was also observed in DMSO samples Lipogems® *vs.* Lipoaspirate; however, signs of increased glucose availability (increases in glucose, fructose and an isobar of mannitol/sorbitol) with increases in pyruvate and lactate were also observed, which could suggest changes in energy demand in this comparison. NAD+ and related metabolites (e.g., 1-methylnicotinamide,
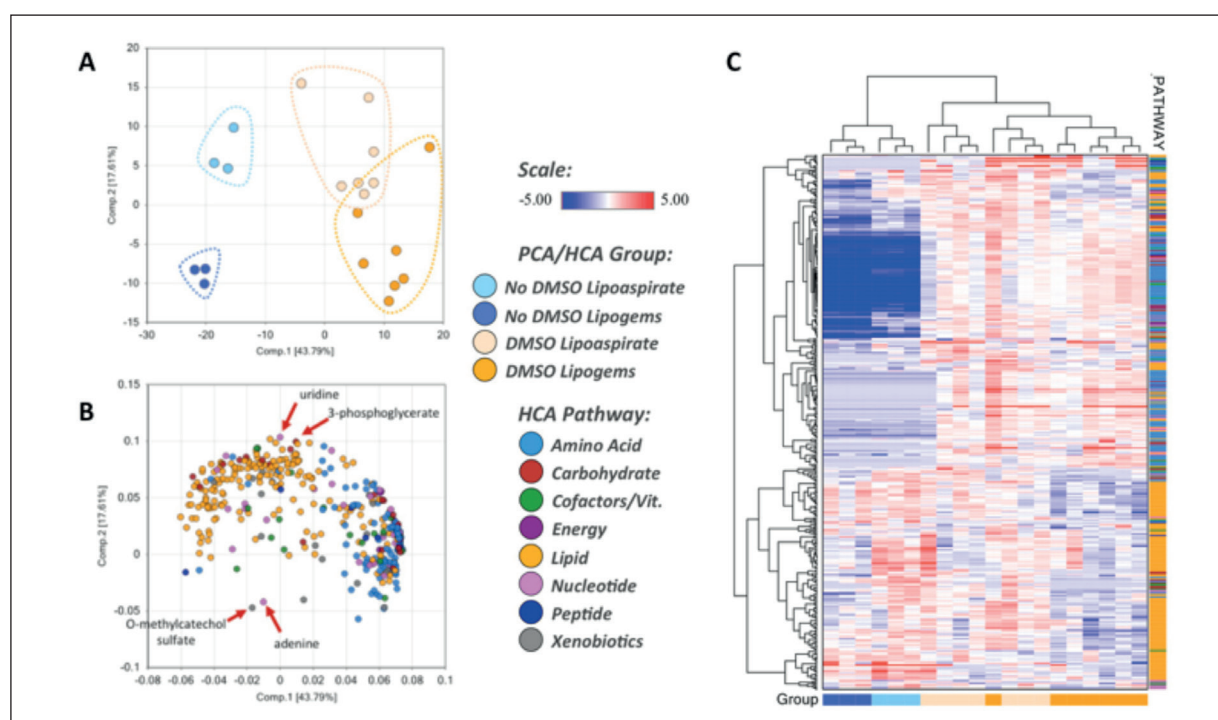
Figure 1. Statistical analysis of metabolomics results separate Lipoaspirate and Lipogems® and DMSO and non-DMSO-treated samples. (**A**) Principal component analysis (PCA) separates the samples when plotted against the first two principal components. (**B**) PCA loadings plot separates the groups in the PCA (**C**) Hierarchical clustering analysis (HCA) separated the samples between DMSO and non-DMSO-treated samples.

N1-methyl-2-pyridon-5- carboxamide) decreased in DMSO and No DMSO, Lipogems® *vs.* Lipoaspirate comparison, consistent with increased glycolytic use (Figure 2).

Lipid Metabolism

Fatty acids are a critical source of energy for mitochondrial oxidation and cellular ATP generation (in addition to being precursors for phospholipids and storage lipids). Long- chain (e.g., palmitate, palmitoleate, margarate) and polyunsaturated (e.g., linoleate, linolenate) fatty acids tended to decline in Lipogems® compared to Lipoaspirate (both DMSO and Non-DMSO fresh frozen tissue), which could suggest changes in use to support energetics (or biosynthetic demand). Long-chain fatty acids must be conjugated to carnitine for efficient transport across the mitochondrial membrane; acylcarnitines also tended to decrease, though not all observed changes achieved significance, which could suggest changes in lipid oxidation. However, the ketone body 3-hydroxybutyrate (BHBA) was not significantly changed – curiously, ketone bodies were not observed in No DMSO-treated samples, which could suggest DMSO altered use (or

uptake/generation) of ketone bodies. Complex lipids (e.g., 1,2-dipalmitoyl-GPC), plasmalogens (e.g., 1-(1-enyl-palmitoyl)-2-oleoyl-GPE), sphingolipids (e.g., N-palmitoyl-sphinganine) and ceramides also tended to decrease in DMSO (Post Pre). Subtle declines in many of these classes in No DMSO (Lipogems® *vs.* Lipoaspirate) did not achieve significance (which may reflect decreased power in these comparisons compared to DMSO-treated comparisons) (Figure 3).

TCA Cycle

Carbon can flow into the TCA cycle from a number of sources, including carbohydrates and lipids (via conversion of acetyl-CoA to citrate), glutamine (entering as alpha- ketoglutarate), and branched-chain amino acids (entering as citrate and succinyl-CoA). Declines in citrate in No DMSO fresh frozen (Lipogems® *vs.* Lipoaspirate) could be consistent with increased acetyl CoA demand (or possibly limiting input from glycolysis), with declines in malate also observed. DMSO (Lipogems® *vs.* Lipoaspirate) did not show a similar trend; however, increases in aconitate [cis or trans] may be consistent with declining energy demand (which was also reflect in glycolytic metabolites) (Figure 4).
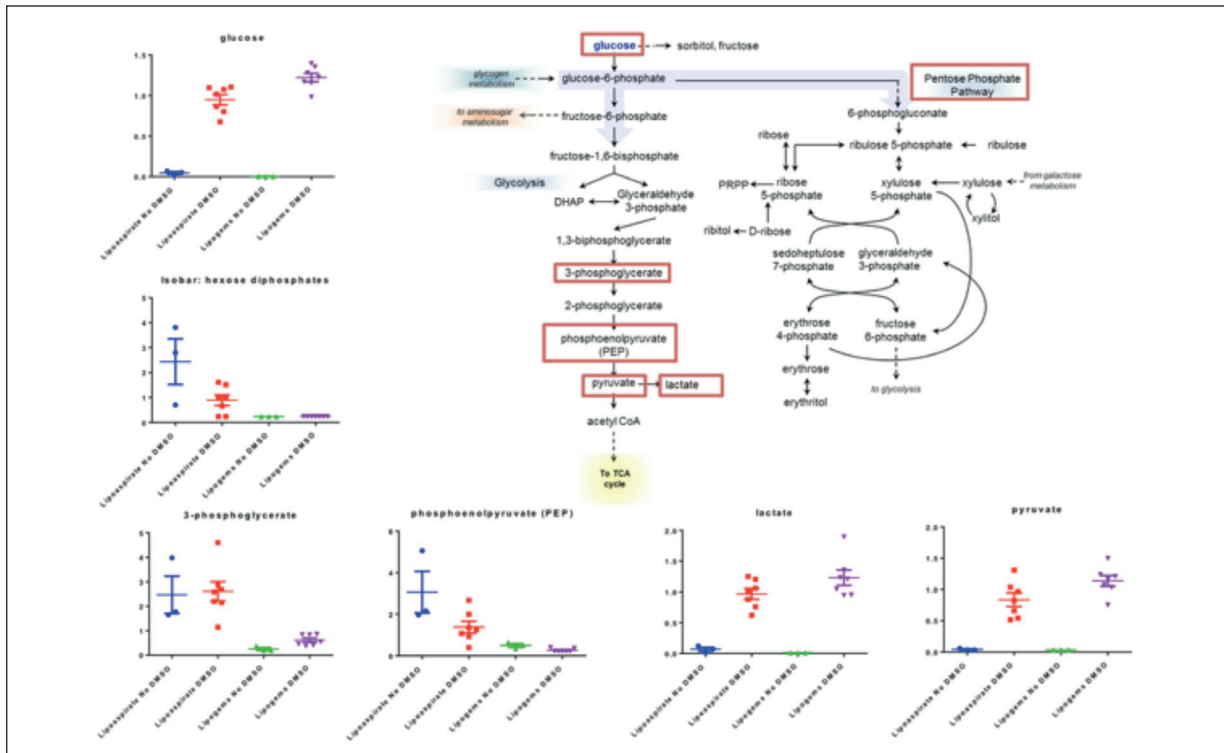
Figure 2. Carbohydrate metabolism. Glycolytic use is increased in microfractured adipose tissue Lipogems® samples compared to non-microfractured Lipoaspirate adipose tissue. The y-axis for glucose is plotted on a log-scale to better show population distributions in the box plot.
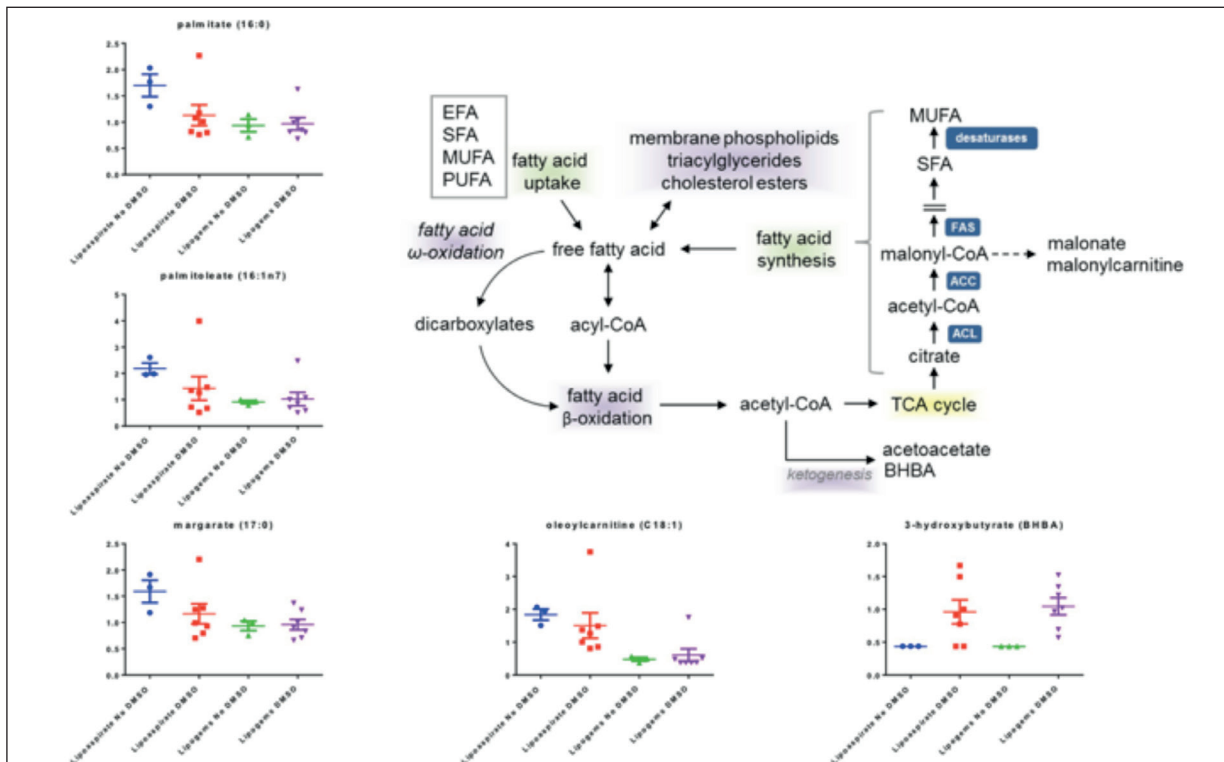
Figure 3. Lipid metabolism. Fatty acids are decline in in microfractured adipose tissue Lipogems samples compared to non-microfractured Lipoaspirate adipose tissue.
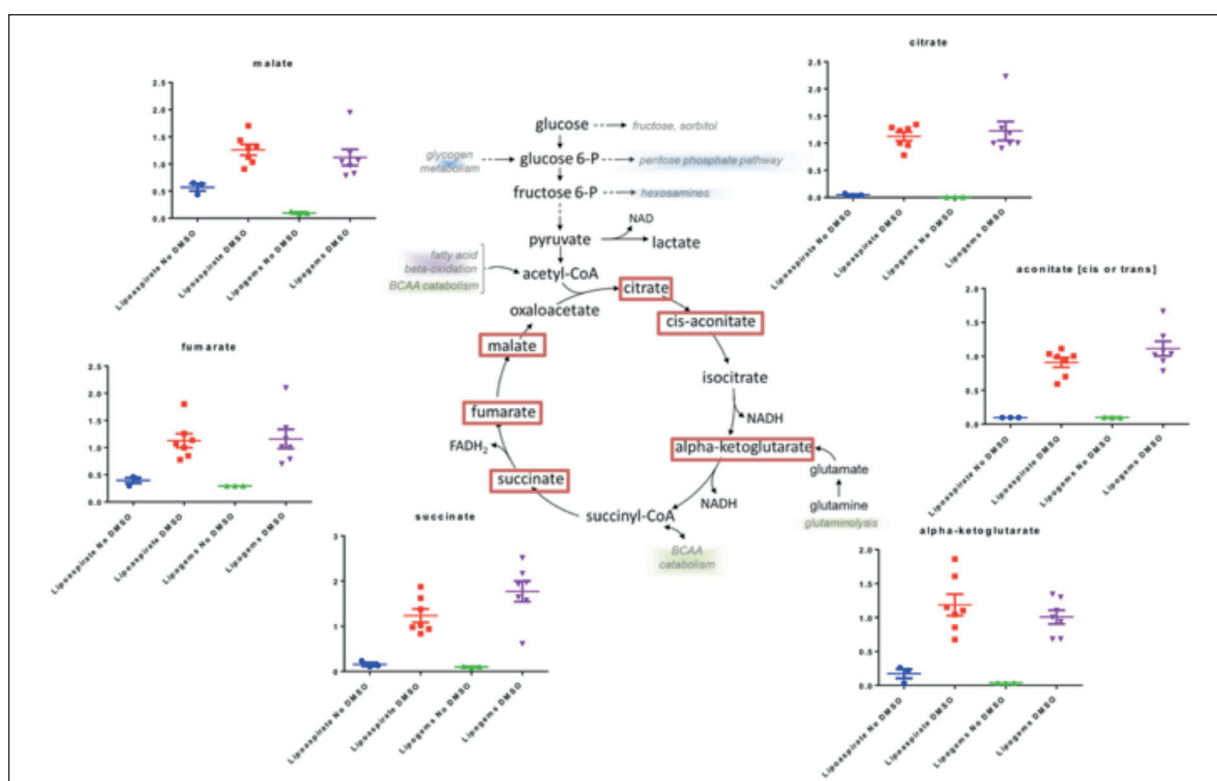
Figure 4. TCA cycle. The y-axis in citrate is plotted against a log-scale to better show population distribution.

Changes in Amino Acid Metabolism/Availability

Amino acid metabolites tended to show divergent trends in the DMSO-treated and non- DMSO fresh frozen comparisons. In the DMSO-treated comparison (DMSO, Lipogems® *vs.* Lipoaspirate), amino acids (e.g., Gly, Ser, Ala, Glu, Gln, His) and their catabolite tended to increase. However, in the non-DMSO fresh frozen comparison (No DMSO, Lipogems® *vs.* Lipoaspirate), amino acids and their catabolites tended to decline as a class. Changes in amino acid metabolites can reflect differences in biosynthetic demand when considered together, with patterns associated with declining energy demand above (Table III).

Bile Acids

Primary and secondary bile acids tended to increase as a class in DMSO (Lipogems® *vs.* Lipoaspirate); interestingly, these biochemicals were below the threshold of detection in non-DMSO fresh frozen samples. DMSO has been shown to increase membrane permeability, which may aid transport of bile acids (or potentially enhance extraction from cells during processing).

Nucleotide Metabolism

Declines in purine catabolites (e.g., hypoxanthine, xanthine) could suggest changes in nucleotide demand (no DMSO, Lipogems® *vs.* Lipoaspirate); adenine was also elevated, with a non-significant increase in adenosine (and a subtle, non-significant decline in AMP), consistent with increased demand. Pyrimidine metabolites showed similar changes, with a decline in orotidine, uridine and uracil consistent with increased demand. Declining nucleotide availability may reflect increased transcriptional use (e.g., activation of stress-responsive pathways) or proliferative demand.

Discussion

Mesenchymal stromal cells (MSCs) have the capacity to differentiate *in-vitro* into a variety of cell types, and have paracrine properties that can assist tissue regeneration and repair, which make them of great interest for regenerative medicine applications[1,5].

Table III. Amino Acids showed divergent trends. Red and green shaded cells indicate $p \leq 0.05$ (red indicates that the mean values are significantly higher for that comparison; green values significantly lower). Light red and light green shaded cells indicate $0.05 < p < 0.10$ (light red indicates that the mean values trend higher for that comparison; light green values trend lower).

Pathway	Biochemical Name	DMSO Lipogems DMSO Lipoaspirate	No DMSO Lipogems No DMSO Lipoaspirate	No DMSO Lipoaspirate DMSO Lipoaspirate	No DMSO Lipogems DMSO Lipogems
Glycine, Serine and Threonine Metabolism	G glycine	1.25	0.34	0.17	0.05
	N-acetylglycine	1.70	0.93	0.68	0.42
	dimethylglycine	1.47	1.00	0.56	0.40
	betaine	1.27	0.36	0.16	0.04
	serine	1.25	0.37	0.28	0.08
	N-acetylserine	0.97	0.45	0.82	0.37
	threonine	1.34	0.30	0.11	0.02
	N-acetylthreonine	1.49	0.69	0.27	0.11
Alanine and Aspartate Metabolism	alanine	1.28	0.28	0.07	0.02
	N-acetylalanine	0.99	0.82	0.49	0.40
	aspartate	1.26	0.53	0.13	0.06
	N-acetylaspartate (NAA)	1.39	0.56	0.70	0.51
	asparagine	1.29	0.24	0.15	0.03
	N-acetylasparagine	1.42	1.00	0.69	0.51
Glutamate Metabolism	glutamate	1.25	0.22	0.16	0.03
	glutamine	1.38	0.15	0.03	0.00
	N-acetylglutamate	0.62	0.80	1.02	1.11
	N-acetylglutamine	1.59	1.00	0.53	0.36
	4-hydroxyglutamate	1.49	1.00	0.75	0.53
	glutamate, gamma-methyl ester	1.06	1.00	0.58	0.55
	pyroglutamine*	1.36	0.22	0.57	0.10
	beta-citrylglutamate	0.43	0.32	0.66	0.42
Histidine Metabolism	histidine	1.46	0.19	0.11	0.01
	1-methylhistidine	1.60	1.00	0.52	0.33
	3-methylhistidine	1.51	1.00	0.49	0.36
	N-acetylhistidine	1.41	1.00	0.79	0.57
	hydantoin-5-propionic acid	1.51	1.00	0.58	0.40
	trans-urocanate	1.23	0.84	0.36	0.26
	imidazole propionate	1.32	1.00	0.68	0.55
	imidazole lactate	1.42	0.83	0.85	0.50
	carnosine	1.54	1.00	0.51	0.34
	histamine	0.56	0.91	0.40	0.58
	1-methylimidazoleacetate	0.77	0.32	0.51	0.20
	4-imidazoleacetate	0.44	0.16	0.66	0.24
Lysine Metabolism	lysine	1.32	0.38	0.17	0.05
	N6,N6,N6-trimethyllysine	1.61	0.84	0.04	0.02
	5-hydroxylysine	1.51	1.00	0.42	0.29
	5-(galactosylhydroxy)-L- lysine	1.18	0.92	0.27	0.21
	2-aminoadipate	1.27	0.57	0.39	0.18
	glutarate (pentanedioate)	1.30	1.16	0.18	0.17
	pipecolate	1.06	0.66	0.64	0.47
	6-oxopiperidine-2- carboxylate	1.45	1.00	0.58	0.42
Phenylalanine and Tyrosine Metabolism	phenylalanine	1.32	0.34	0.13	0.03
	N-acetylphenylalanine	1.48		0.78	0.54
	tyrosine	1.37	0.34	0.14	0.04
	N-acetyltyrosine	1.24	1.00	0.76	0.62
	3-(4-hydroxyphenyl)lactate	1.35	1.00	0.11	0.08
	phenol sulfate	0.84	0.19	0.62	0.15
	p-cresol sulfate	0.98	0.43	0.20	0.03
	o-Tyrosine	1.21	1.00	0.82	0.70
	N-formylphenylalanine	1.38	1.00	0.44	0.34

Continued

Table III. Amino acids showed divergent trends. Red and green shaded cells indicate $p \leq 0.05$ (red indicates that the mean values are significantly higher for that comparison; green values significantly lower). Light red and light green shaded cells indicate $0.05 < p < 0.10$ (light red indicates that the mean values trend higher for that comparison; light green values trend lower).

Pathway	Biochemical Name	DMSO Lipogems DMSO Lipoaspirate	No DMSO Lipogems No DMSO Lipoaspirate	No DMSO Lipoaspirate DMSO Lipoaspirate	No DMSO Lipogems DMSO Lipogems
Tryptophan metabolism	tryptophan	1.36	0.23	0.14	0.02
	3-indoxyl sulfate	0.96	0.72	0.65	0.42
	indolelactate	1.57	1.00	0.48	0.32
	kynurenine	1.14	0.44	0.27	0.05
	kynurenate	1.41	1.00	0.75	0.54
	5-hydroxyindoleacetate	1.66	1.00	0.68	0.42
	C-glycosyltryptophan	1.18	1.00	0.58	0.49
Leucine, Isoleucine and Valine metabolism	leucine	1.30	0.36	0.13	0.04
	N-acetylleucine	1.82	1.00	0.96	0.54
	4-methyl-2-oxopentanoate	0.77	0.83	0.37	0.57
	isovalerylglycine	1.60	1.00	0.25	0.20
	isovalerylcarnitine (C5)	0.31	0.15	0.67	0.52
	beta-hydroxyisovalerate	1.18	1.00	0.49	0.44
	3-methylglutaconate	1.49	1.00	0.79	0.54
	isoleucine	1.36	0.40	0.05	0.02
	N-acetylisoleucine	1.90	1.00	0.53	0.31
	3-methyl-2-oxovalerate	0.69	0.94	0.42	0.59
	alpha-hydroxyisovalerate	1.13	1.00	0.45	0.41
	2-methylbutyrylcarnitine (C5)	0.98	1.00	0.78	0.84
	2-methylbutyrylglycine	1.38	1.00	0.60	0.45
	ethylmalonate	1.57	1.00	0.74	0.47
	methylsuccinate	1.44	1.02	0.08	0.06
	valine	1.34	0.18	0.11	0.01
	isobutyrylcarnitine (C4)	1.36	0.68	0.14	0.06
	3-hydroxyisobutyrate	1.64	1.00	0.80	0.52
Methionine, Cysteine, SAM and Taurine metabolism	methionine	1.28	0.54	0.20	0.09
	N-acetylmethionine	0.65	0.63	0.69	0.69
	methionine sulfone	1.62	1.00	0.68	0.42
	methionine sulfoxide	1.40	0.76	0.10	0.05
	cystathionine	1.30	1.00	0.57	0.43
	cysteine	1.30	0.12	0.08	0.01
	S-methylcysteine	0.94	0.85	0.19	0.17
	cysteine s-sulfate	1.81	1.00	0.40	0.24
	cystine	1.64	0.78	0.02	0.01
	cysteine sulfinic acid	1.35	0.88	0.11	0.07
	hypotaurine	0.94	0.68	0.53	0.34
	taurine	0.28	0.20	2.15	1.53
	N-acetyltaurine	1.43	1.00	0.06	0.04
	2-hydroxybutyrate/2-hydroxyisobutyrate	1.20	0.70	0.50	0.31
Urea cycle; Arginine and Proline Metabolism	arginine	1.34	0.44	0.15	0.05
	urea	1.24	0.50	0.30	0.11
	ornithine	1.40	0.34	0.14	0.03
	2-oxoarginine*	1.58	1.00	0.68	0.45
	citrulline	1.24	0.29	0.21	0.05
	homoarginine	1.57	1.00	0.64	0.42
	proline	1.28	0.22	0.12	0.02
	dimethylarginine (SDMA + ADMA)	1.15	0.89	0.26	0.20
	N-acetylarginine	1.66	1.00	0.41	0.28
	N-delta-acetylornithine	1.31	1.00	0.32	0.27
	trans-4-hydroxyproline	1.27	0.14	0.09	0.01
	pro-hydroxy-pro	1.45	1.00	0.52	0.36
	N-methylproline	1.39	1.00	0.70	0.51

Continued

Table III. Amino acids showed divergent trends. Red and green shaded cells indicate $p \leq 0.05$ (red indicates that the mean values are significantly higher for that comparison; green values significantly lower). Light red and light green shaded cells indicate $0.05 < p < 0.10$ (light red indicates that the mean values trend higher for that comparison; light green values trend lower).

Pathway	Biochemical Name	DMSO Lipogems DMSO Lipoaspirate	No DMSO Lipogems No DMSO Lipoaspirate	No DMSO Lipoaspirate DMSO Lipoaspirate	No DMSO Lipogems DMSO Lipogems
Creatine metabolism	guanidinoacetate	0.78	0.26	0.55	0.17
	creatine	0.63	0.28	1.03	0.47
	creatinine	1.27	0.25	0.24	0.05
	creatine phosphate	0.39	0.16	1.76	0.68
Polyamine metabolism	spermidine	0.75	0.33	0.50	0.18
	spermine	1.25	1.00	0.44	0.37
	4-acetamidobutanoate	1.48	0.94	0.11	0.07
Glutathione metabolism	glutathione, reduced (GSH)	1.00	1.23	2.39	2.33
	glutathione, oxidized (GSSG)	0.43	0.16	4.48	2.17
	cysteine-glutathione disulfide	0.47	0.34	0.17	0.10
	5-oxoproline	1.50	0.55	0.07	0.02
	ophthalmate	0.85	0.55	1.64	1.00

Several groups have suggested that adipose tissue may be an ideal source for MSCs, though methods of isolation involve extensive *ex-vivo* processing[23] (e.g., enzymatic digestion and expansion), which can affect differentiation potential and limit mulitipotency[11]. Recently, Lipogems® International has introduced a protocol to obtain microfragmented adipose tissue products with intact stromal vascular niches (which may maintain hADSCs multipotency). Lipogems processing significantly reduces contaminating blood, removes lipids and other cytosolic components resulting from damage to the tissue during collection of the lipoaspirates and results in a microfractured tissue enriched in stem cells and pericytes compared with the unprocessed lipoaspirates[13,14]. This study assessed lipoaspirate tissue and Lipogems® microfractured adipose tissue, either exposed to DMSO for cryopreservation or fresh-frozen without DMSO, with the goal of identifying possible metabolomic differences between adipose tissue products and cryopreservation methods.

Comparison of global biochemical profiles in adipose (either exposed to DMSO or not) revealed several metabolomic differences including changes in metabolites related to the amino acid metabolism and energetics. Several common differences were observed in both DMSO and non-DMSO fresh frozen samples (Lipogems® *vs.* Lipoaspirate), including changes in carbohydrate and nucleotide metabolism. Signs of shifts toward increasing glycolytic use may reflect enrichment of mesenchymal stem cells in microfractured adipose tissue Lipogems® sample[24,25], with patterns associated with increasing nucleotide demand consistent with the highly proliferative nature of these cells[26].

Amino acid metabolites, however, tended to show divergent changes between DMSO and non-DMSO comparisons, which could reflect changes in cellular uptake/transport or contributions from DMSO storage solution (or a combination of both) as previously reported[26,28].

Conclusions

Collectively, our findings suggest that the Lipogems system modifies the metabolic profile of lipoaspirate tissues products. Further work will be needed to determine the specific mechanisms involved in the observed metabolic changes associated with tissue processing. Finally, studies assessing the "stemness" of cells exposed to DMSO could be of assistance to identify possible effects of the cryopreservation method on hADSCs differentiation potential and paracrine effects in target tissues.

Conflict of Interest

Camillo Ricordi is a founding scientist and a member of the scientific advisory board of Lipogems International SpA. Armando J. Mendez received funding for studies from Lipogems. The other authors declare that they have no financial competing interests.

References

1) Zuk PA, Zhu M, Ashjian P, De Ugarte DA, Huang JI, Mizuno H, Alfonso ZC, Fraser JK, Benhaim P, Hedrick MH. Human adipose tissue is a source of multipotent stem cells. Mol Biol Cell 2002; 13: 4279-4295.

2) Liang X, Ding Y, Zhang Y, Tse HF, Lian Q. Paracrine mechanisms of mesenchymal stem cell-based therapy: current status and perspectives. Cell Transplant 2014; 23: 1045-1059.

3) Tan SS, Yin Y, Lee T, Lai RC, Yeo RW, Zhang B, Choo A, Lim SK. Therapeutic MSC exosomes are derived from lipid raft microdomains in the plasma membrane. J Extracell Vesicles 2013 Dec 23; 2. doi: 10.3402/jev.v2i0.22614. eCollection 2013.

4) García-Contreras M, Messaggio F., Jimenez O, Mendez A. differences in exosome content of human adipose tissue processed by non-enzymatic and enzymatic methods. CellR4 2015; 3: e1423.

5) Gimble JM, Bunnell BA, Guilak F. Human adipose-derived cells: an update on the transition to clinical translation. Regen Med 2012; 7: 225-235.

6) García-Contreras M, Vera-Donoso CD, Hernández-Andreu JM, García-Verdugo JM, Oltra E. Therapeutic potential of human adipose-derived stem cells (ADSCs) from cancer patients: a pilot study. PLoS One 2014; 9: e113288.

7) Puglisi MA, Saulnier N, Piscaglia AC, Tondi P, Agnes S, Gasbarrini A. Adipose tissue-derived mesenchymal stem cells and hepatic differentiation: old concepts and future perspectives. Eur Rev Med Pharmacol Sci. 2011; 15(4):355-64.

8) Pu LL, Cui X, Fink BF, Gao D, Vasconez HC. Adipose aspirates as a source for human processed lipoaspirate cells after optimal cryopreservation. Plast Reconstr Surg 2006; 117: 1845-1850.

9) Choudhery MS, Badowski M, Muise A, Pierce J, Harris DT. Cryopreservation of whole adipose tissue for future use in regenerative medicine. J Surg Res 2014; 187: 24-35.

10) Cui XD, Gao DY, Fink BF, Vasconez HC, Pu LL. Cryopreservation of human adipose tissues. Cryobiology 2007; 55: 269-278.

11) Aronowitz JA, Lockhart RA, Hakakian CS. Mechanical versus enzymatic isolation of stromal vascular fraction cells from adipose tissue. Springerplus 2015; 4: 713.

12) Oberbauer E, Steffenhagen C, Wurzer C, Gabriel C, Redl H, Wolbank S. Enzymatic and non-enzymatic isolation systems for adipose tissue-derived cells: current state of the art. Cell Regen (Lond)

2015 Sep 30;4:7. doi: 10.1186/s13619-015-0020-0. eCollection 2015.

13) Carelli S, Messaggio F, Canazza A, Hebda DM, Caremoli F, Latorre E, Grimoldi MG, Colli M, Bulfamante G, Tremolada C, Di Giulio AM, Gorio A. Characteristics and properties of mesenchymal stem cells derived from microfragmented adipose tissue. Cell Transplant 2015; 24: 1233-1252.

14) Bianchi F, Maioli M, Leonardi E, Olivi E, Pasquinelli G, Valente S, Mendez AJ, Ricordi C, Raffaini M, Tremolada C, Ventura C. A new nonenzymatic method and device to obtain a fat tissue derivative highly enriched in pericyte-like elements by mild mechanical forces from human lipoaspirates. Cell Transplant 2013; 22: 2063-2077.

15) Randelli P, Menon A, Ragone V, Creo P, Bergante S, Randelli F, De Girolamo L, Alfieri Montrasio U, Banfi G, Cabitza P, Tettamanti G, Anastasia L. Lipogems product treatment increases the proliferation rate of human tendon stem cells without affecting their stemness and differentiation capability. Stem Cells Int 2016; 2016: 4373410.

16) Bosetti M, Borrone A, Follenzi A, Messaggio F, Tremolada C, Cannas M. Human lipoaspirate as autologous injectable active scaffold for one-step repair of cartilage defects. Cell Transplant 2016; 25: 1043-1056.

17) Bianchi F, Olivi E, Baldassarre M, Giannone FA, Laggetta M, Valente S, Cavallini C, Tassinari R, Canaider S, Pasquinelli G, Tremolada C, Ventura C. Lipogems, a new modality of fat tissue handling to enhance tissue repair in chronic hind limb ischemia. CellR4 2014; 2: e1289.

18) Giori A, Tremolada C, Vailati R, Navone SE, Marfia G, Caplan AI. Recovery of function in anal incontinence after micro-fragmented fat graft (Lipogems®) injection: two years follow up of the first 5 cases. CellR4 2015; 2: e1544.

19) Naka K, Jomen Y, Ishihara K, Kim J, Ishimoto T, Bae EJ, Mohney RP, Stirdivant SM, Oshima H, Oshima M, Kim DW, Nakauchi H, Takihara Y, Kato Y, Ooshima A, Kim SJ. Dipeptide species regulate p38MAPK-Smad3 signalling to maintain chronic myelogenous leukaemia stem cells. Nat Commun 2015; 6: 8039.

20) Solini A, Manca ML, Penno G, Pugliese G, Cobb JE, Ferrannini E. Prediction of declining renal function and albuminuria in patients with type 2 diabetes by metabolomics. J Clin Endocrinol Metab 2016; 101: 696-704.

21) L., B., Random forests. Machine Learning 2001; 45: 5-32.

22) Shannon P, Markiel A, Ozier O, Baliga NS, Wang JT, Ramage D, Amin N, Schwikowski B, Ideker T. Cytoscape: a software environment for integrated models of biomolecular interaction networks. Genome Res 2003; 13: 2498-5204.

23) Raposio E, Bertozzi N. How to isolate a ready-to-use adipose-derived stem cells pellet for clinical application. Eur Rev Med Pharmacol Sci. 2017;21:4252-4260.

24) Schop D, Janssen FW, van Rijn LD, Fernandes H, Bloem RM, de Bruijn JD, van Dijkhuizen-Radersma R. Growth, metabolism, and growth inhibitors

of mesenchymal stem cells. Tissue Eng Part A 2009; 15: 1877-1886.

25) Mischen BT, Follmar KE, Moyer KE, Buehrer B, Olbrich KC, Levin LS, Klitzman B, Erdmann D. Metabolic and functional characterization of human adipose-derived stem cells in tissue engineering. Plast Reconstr Surg 2008; 122: 725-738.

26) Ito K, Suda T. Metabolic requirements for the maintenance of self- renewing stem cells. Nat Rev Mol Cell Biol 2014; 15: 243-256.

27) Almeida MM, Caires LC, Musso CM, Campos JM, Maranduba CM, Macedo GC, Mendonça JP, Garcia RM. Protocol to cryopreserve and isolate nuclei from adipose tissue without dimethyl sulfoxide. Genet Mol Res 2014; 13: 10921-10933.

28) Naaldijk Y, Staude M, Fedorova V, Stolzing A. Effect of different freezing rates during cryopreservation of rat mesenchymal stem cells using combinations of hydroxyethyl starch and dimethylsulfoxide. BMC Biotechnol 2012; 12: 49.